

# Microwave detection up to 43.5 GHz by GaN nano-diodes: Experimental and analytical responsivity

H. Sánchez-Martín, S. Sánchez-Martín,  
O. García-Pérez, S. Pérez, J. Mateos,  
T. González, and I. Íñiguez-de-la-Torre

Departamento de Física Aplicada, Universidad de  
Salamanca, Plaza de la Merced s/n, 37008 Salamanca, Spain  
e-mail: hectorsanchezmartin@usal.es

C. Gaquière

Institut d'Électronique, Microélectronique et de  
Nanotechnologies (IEMN), Villeneuve D'Ascq, France

**Abstract**— Planar nano-diodes fabricated on an AlGaN/GaN heterolayer have been measured, showing capability to detect microwave signals up to 43.5 GHz at room temperature. A single nano-diode with length  $L=1000$  nm and width  $W=74$  nm provides a response of approximately 55 mV DC output for a 0 dBm nominal input power at 1 GHz, with a very small fraction of the RF power reaching effectively the device due to a very large impedance mismatch. A comprehensive analytical study, which uses as input data just the measured DC current-voltage curve of the diodes, is able to replicate the values of the RF characterization and allows a deep understanding of the detection mechanism.

**Keywords**— AlGaN/GaN; terahertz; self-switching diode; detector; zero-bias detector

## I. INTRODUCTION

The device under study in this paper, demonstrated in 2003 by Aimin Song et al. [1], is the so-called self-switching diode (SSD). The SSD be made up of a conductive nano-channel created by an L-shaped etched pattern of isolating regions. The device principle was explained in terms of electrostatic effect as that of a field-effect transistor together with the surface depletion in the boundaries of the trenches. The asymmetry of the layout makes possible that the flanges act as lateral gates opening/closing the nano-channel. Thus, an attractive non-linear I-V curve is created.

SSDs have been investigated in several applications. Here, we explore its promising performance to be used as an efficient solid-state direct detector from microwave up to the terahertz regime [2]. Compared with other technologies, the SSD has three main advantages: (i) just one nanolithography step is needed in their fabrication to create insulating trenches in the semiconductor layers, (ii) it is a planar device so that a group of them can be arranged as focal plane arrays, and (iii) when realized with high mobility semiconductors they can reach operation frequencies in the THz range at room temperature as predicted by means of Monte Carlo simulations solving Boltzmann's transport equation in the time domain [3]. In addition, the use of a wide band gap semiconductor like GaN allows forecasting capability for very high power detection [4].

In this work, we report on detection experiments up to 43.5 GHz performed in GaN SSDs and show how an analytical model, which takes as input data the DC I-V curve of the

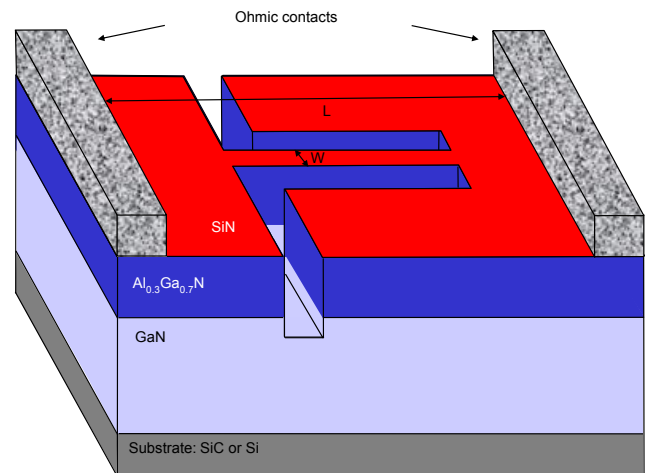


Fig. 1. Schematic diagram of the heterostructure of the device. Two L-Shaped etched trenches define an asymmetric channel.

diodes, is able to predict the responsivity of the devices. The fact that the information contained in the DC I-V curve is enough to predict the RF responsivity means that the AC response of the diodes follows essentially the DC behavior,

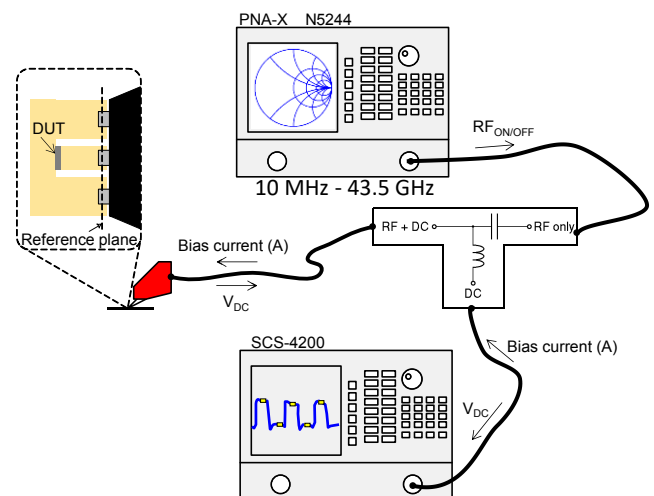


Fig. 2. Schematic diagram of the microwave experimental setup. A probe station connected to a semiconductor analyzer Keithley 4200 SCS and a vector network analyzer PNA-X N5244 through a bias-tee.

This work has been partially supported by the Ministerio de Economía y Competitividad (Dirección General de Investigación) through the project TEC2013-41640-R and the Junta de Castilla y León through the project SA022U16.

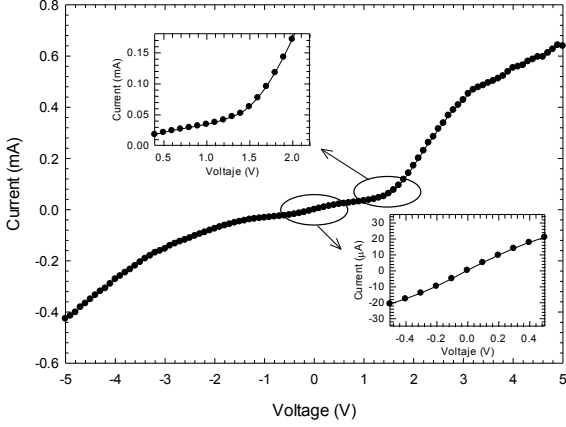


Fig. 3. Current-voltage characteristic of an SSD with  $L=1000$  nm and  $W=74$  nm. Inset: Zoom of the zero bias area and that around 1.3 V.

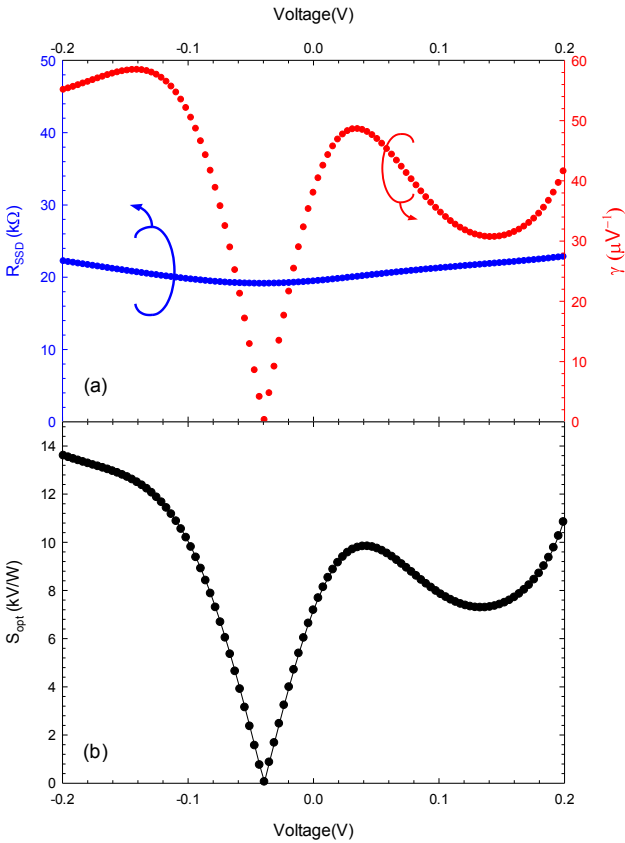


Fig. 4. (a) Impedance (left axis) and absolute value of the bow factor (right axis) extracted from the I-V curve of the SSD. Fig. 4(b) Responsivity in V/W calculated using  $S_{opt} = \gamma / 2R_{SSD}$ .

what happens not only up to the 43.5 GHz limit of our setup, but up to hundreds of GHz [2,4].

## II. DEVICE AND EXPERIMENTAL SETUP

The tested SSDs are based on an epitaxial layer consisting of  $1.8 \mu\text{m}$  of GaN on Si substrate, with an  $\text{Al}_{0.3}\text{Ga}_{0.7}\text{N}$  barrier

of 23 nm as shown in Fig. 1. The carrier density of the 2DEG and mobility at room temperature are  $n_s=6 \times 10^{12} \text{ cm}^{-2}$  and  $\mu=1200 \text{ cm}^2/\text{V s}$ , respectively. Design parameters are channel width ( $W$ ) and length ( $L$ ). The experimental set-up is presented in Fig. 2. Measurements were carried out using a vector network analyzer model PNA X N5244A from Keysight Technologies, in the frequency range between 10 MHz and 43.5 GHz (but the results presented can be extended to the near THz range [5, 6]) and a semiconductor characterization system model 4200 SCS from Keithley. The SSDs were contacted using coplanar probes in the ground-signal-ground (GSG) configuration to ensure a good microwave coupling. To estimate the power delivered to the DUT at the reference plane, the losses due to cables, connectors and probes are taken into account. The PNA was used as the microwave generator. By means of a bias-tee, different biases, by means of DC currents, are applied with the SCS. The detected DC voltage was measured by switching on and off the RF signal, and recording the difference in the DC output voltage generated by the SSD array due to the RF signal waves.

## III. ANALYTICAL RESPONSIVITY

Under small-signal conditions, the SSD should operate as a square-law detector. Basically, the direct detection is based on the following principle. If we apply an incident power,  $P_{in}$ , on the detector, it causes a shift in the voltage  $\Delta V$  across the device. The ratio  $\Delta V/P_{in}$  is called voltage responsivity. The microwave detection responsivity of any electronic nonlinear device is determined by the nonlinearity in its current-voltage characteristic [7]. Therefore, by means of a detailed inspection of the I-V curve, it is possible to predict the measurements of responsivity in V/W. This analysis may help in the future to select, just with a fast DC test, the appropriate device to be characterized in detail in RF. By means of a Taylor expansion of the current, it is easy to calculate the open circuit detected voltage, which is proportional to the input RF power and the second derivative of the I-V curve, and inversely proportional to the conductance. As usual, at high frequencies, a mismatch between the input and the DUT impedance induces power reflection and different results for responsivity. The calculated responsivity in V/W for an optimal matching between the input and the device impedance is:

$$S_{opt} = \frac{1}{2} R_{SSD} \gamma, \quad (1)$$

where  $R_{SSD}$  is the differential intrinsic resistance at the DC operating point and  $\gamma$  is the bow factor, defined as:

$$\gamma = \frac{d^2 I}{dV^2} \bigg/ \frac{dI}{dV}. \quad (2)$$

However, this optimal or intrinsic magnitude has to be corrected using the reflection coefficient to extract the extrinsic value of the responsivity ( $S$ ) in mismatching between the input and the device impedance, as

$$S = S_{opt}(1 - |\Gamma|^2), \quad (3)$$

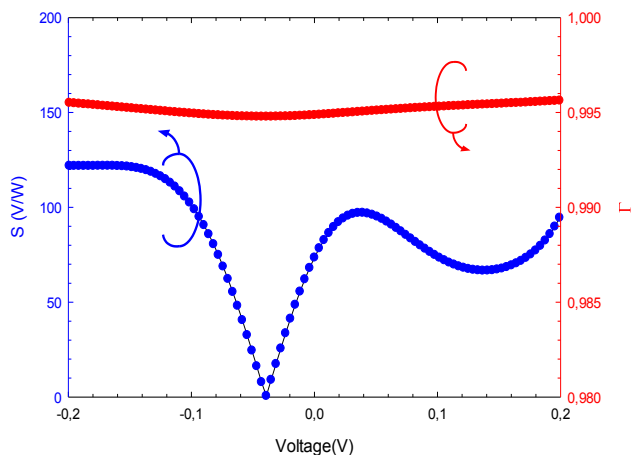


Fig. 5. Responsivity in V/W calculated using  $S=S_{opt}(1-|\Gamma|^2)$  (left axis) and value of the reflection coefficient (right axis).

where

$$\Gamma = \frac{R_{SSD} - R_0}{R_{SSD} + R_0} \quad (4)$$

is the reflection coefficient, with  $R_0$  the characteristic resistance of the access line. The described analytical model is applied to the experimental I-V curve of Fig. 3, where the insets show a zoom of the areas of interest for a fitting of the curve. By means of a 5<sup>th</sup> order polynomial fitting it is easy to

compute the values of  $R_{SSD}$  and  $\gamma$ , Fig. 4(a). Note that at 0 A the bow factor  $\gamma$  is about  $35 \mu\text{V}^{-1}$ , while the impedance is around  $20 \text{ k}\Omega$ , much higher than the  $50 \Omega$  of the access line. Because of this large impedance mismatch the reflection is huge, with values of  $\Gamma$  close to 1, what means that almost 99% of the incident power is reflected, see Fig. 5. Fig. 4(b) presents the calculated values for the responsivity with an optimal RF-match in the vicinity of zero bias, with a value of  $7 \text{ kV/W}$ . With this responsivity and the reflection coefficient of Fig. 5, it is possible to calculate the extrinsic responsivity in the order of 10's of V/W. A similar study can be done for any bias point in the current-voltage curve. Top left inset of Fig. 3 shows the elbow (higher non-linearity) in the I-V curve to be the optimal one for detection properties. Calculations provide a  $S_{opt}$  (or intrinsic responsivity) around  $12 \text{ kV/W}$ , and the extrinsic responsivity  $S$ , around  $200 \text{ V/W}$ .

In addition to the DC voltage ( $\Delta V$ ) induced by the presence of the RF signal, a noise voltage is always present across the device, which in case of being of the same amplitude of  $\Delta V$  makes the detection unfeasible. Considering only Johnson-Nyquist noise (device operating at zero bias), the minimum detectable power per square root bandwidth of a detector, without an optimum losses match and when the diode is driven by a limited source impedance, is called noise equivalent power (NEP) and is calculated as:

$$NEP = \sqrt{4kTR_{SSD}} / S, \quad (5)$$

where  $R_{SSD}$  is the zero-bias resistance. For the SSD under analysis, the value of the NEP is about  $200 \text{ pW/Hz}^{1/2}$ .

#### IV. EXPERIMENTAL RESPONSIVITY

A detailed inspection of the I-V curve and its derivatives suggests that the highest nonlinearity appears at around  $45 \mu\text{A}$ . Therefore, the measurements were done at both biasing conditions, 0 A and  $45 \mu\text{A}$  (corresponding to  $1.3 \text{ V}$ ). The input power of the injected RF signal ranges from  $-10$  to  $10 \text{ dBm}$  and the frequency from  $100 \text{ MHz}$  up to  $43.5 \text{ GHz}$ . The input RF signal was chopped with a period of several seconds and the measured voltage was recorded. Fig. 6(a) shows, at a moderate input power of  $0 \text{ dBm}$ , how the responsivity is practically constant in the frequency range of the experimental set-up. An enhancement of  $S$  is observed when biasing the device at  $45 \mu\text{A}$ . Note that the values are in good agreement with the estimation of the analytical model, shown by lines [5]. Fig. 6(b) displays the output voltage vs. the input power at a frequency of  $1 \text{ GHz}$ . At zero bias the SSD follows the so-called square-law (with constant responsivity) up to  $5 \text{ dBm}$ , where the responsivity decreases, as expected by the reduction of the responsivity predicted by the analytical model for large voltage excursions around zero [see Fig. 4(b)].

Fig. 7 shows I-V curves measured in the diode of Fig. 3 when subjected to an RF input power of  $10 \text{ dBm}$  at different frequencies ( $20 \text{ GHz}$ ,  $30 \text{ GHz}$  and  $40 \text{ GHz}$ ), compared to the DC case. The insets show a zoom of the zero-bias and  $1.3 \text{ V}$  areas. As observed, the presence of the RF power leads to a different I-V curve, the responsivity being higher for larger

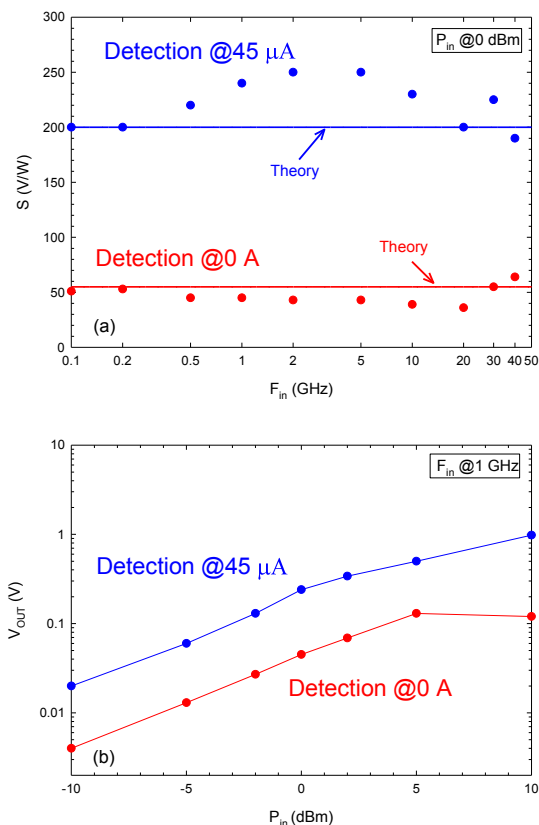


Fig. 6. (a) Frequency response of the SSDs from  $100 \text{ MHz}$  to  $43.5 \text{ GHz}$  at  $0 \mu\text{A}$  ( $0 \text{ V}$ ) and  $45 \mu\text{A}$  bias current, measured with  $0 \text{ dBm}$  input at room temperature. (b) Detected output voltage versus the input power of the  $1 \text{ GHz}$  RF signal.

separation between the DC curve and those measured under RF power. These measurements help identifying the optimum bias points for detection.

A similar analysis was performed for the case of a wider SSD ( $W=200$  nm). Near zero-bias the responsivity  $S$  was found to be lower, below  $10$  V/W, than in the previous narrow SSD, but almost independent of the bias. As shown by (1) and (3), the extrinsic responsivity ( $S$ ) is proportional to the bow factor and the diode impedance but also depends on the reflection coefficient. The higher the diode impedance the higher the value of  $\Gamma$ . A better matching between the input (the standard  $50 \Omega$ ) and device impedances is achieved in the wider diode (in the wider SSD the impedance downs to  $8 \text{ k}\Omega$ ). However, despite the narrower diode is more mismatched, due to the reflection coefficient is higher, such effect is compensated by the higher bow factor and device impedance to provide higher values of extrinsic responsivity.

A systematic study of the dependence of  $S$  on numerous options of device layout design such as number of channels and geometrical dimensions of the channel are the next step to be done.

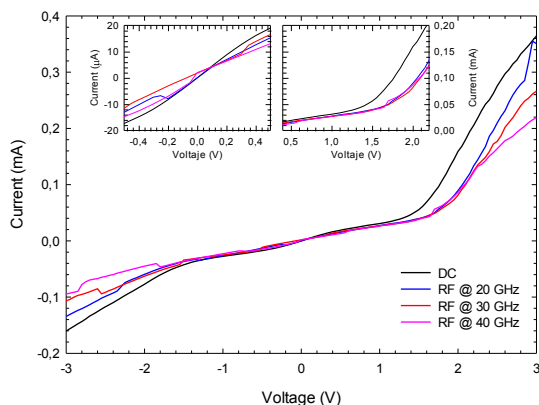


Fig. 7. Current-voltage characteristics measured in the SSD of Fig. 3 when subjected to an input power of  $10$  dBm and different frequencies:  $20$  GHz,  $30$  GHz and  $40$  GHz. The DC case is also shown for comparison. Inset: Zoom of the zero bias area and that around  $1.3$  V.

## V. CONCLUSIONS

An analytical model, that takes the DC I-V data as input, is developed to predict the high frequency responsivity of two terminal detectors. In addition, experimental measurements of the responsivity of nanodiodes fabricated on an AlGaIn/GaN heterolayer have been carried out, obtaining a very good agreement between analytical and experimental data and showing the capability of these devices to detect microwave signals up to  $43.5$  GHz at room temperature.

## REFERENCES

- [1] A. M. Song, M. Missous, P. Omling, A. R. Peaker, L. Samuelson, and W. Seifert, "Unidirectional electron flow in a nanometer-scale semiconductor channel: A self-switching device" *Appl. Phys. Lett.* 83, 1881, 2003.
- [2] C. Balocco, A. M. Song, M. Åberg, A. Forchel, T. González, J. Mateos, I. Maximov, M. Missous, A. A. Rezazadeh, J. Sajjats, L. Samuelson, D. Wallin, K. Williams, L. Worschech, and H. Q. Xu, "Microwave Detection at  $110$  GHz by Nanowires with Broken Symmetry," *Nano Lett.* 5, 1423, 2005.
- [3] J. Mateos, B. G. Vasallo, D. Pardo and T. González T., "Operation and high-frequency performance of nanoscale unipolar rectifying diodes", *Appl. Phys. Lett.* 86, 212103, 2005.
- [4] P. Sangaré, G. Ducournau, B. Grimbert, V. Brandli, M. Faucher, C. Gaquière, A. Íñiguez-de-la-Torre, I. Íñiguez-de-la-Torre, J. F. Milihalter, J. Mateos and T. González, "Experimental demonstration of direct terahertz detection at room-temperature in AlGaIn/GaN asymmetric nanochannels," *J. Appl. Phys.*, vol. 113, pp. 034305, 2013.
- [5] C. Daher, J. Torres, I. Íñiguez-de-la-Torre, P. Nouvel, L. Varani, P. Sangaré, G. Ducournau, C. Gaquière, J. Mateos and T. González, "Room Temperature Direct and Heterodyne Detection of  $0.280.69$ -THz Waves Based on GaN 2-DEG Unipolar Nanochannels," *IEEE Trans. on Electron Devices* 63, 1, 353-359, 2016.
- [6] I. Íñiguez-de-la-Torre et al., "Operation of GaN planar nanodiodes as THz detectors and mixers," *IEEE Trans. Terahertz Sci. Technol.*, vol. 4, no. 6, pp. 670-677, Nov. 2014.
- [7] A. M. Cowley and H. O. Sorensen, "Quantitative comparison of solid-state microwave detectors," *IEEE Trans. Microw. Theory Tech.*, vol. MTT-14, no. 12, pp. 588-602, Dec. 1966